International Journal of Innovative Computing, Information and Control
Volume **8**, Number **5(B)**, May **2012**

ICIC International ©2012 ISSN 1349-4198
pp. 3809–3818

RCS COMPOUND CONTROL DESIGN FOR NEAR SPACE VEHICLES

Yingjing Shi[1], Rui Li[2] and Honglei Xu[3,4]

[1]Institute of Astronautics and Aeronautics
[2]Automation School
University of Electronic Science and Technology of China
No. 2006, Xiyuan Ave., West Gaoxin Dist., Chengdu 611731, P. R. China
{ yingjing.shi; hitlirui }@gmail.com

[3]School of Information Science and Engineering
Central South University
No. 932, South Lushan Rd., Changsha 410083, P. R. China

[4]Department of Mathematics and Statistics
Curtin University of Technology
GPO Box U1987, Perth 6845, Australia
H.Xu@curtin.edu.au

Received October 2010; revised March 2011

Abstract. *In this paper, we consider RCS compound control design problems for near space vehicles. First we analyze the reason for the saturation problem of the elevators of near space vehicles. Based on the analysis results, we propose a class of compound control schemes of elevators and reaction control systems (RCS). In addition, two RCS configuration schemes are provided for the design course. Furthermore, comparisons and analysis of the two classes of RCS thrusters with combination logic and fault reconstruction are presented. By choosing the RCS thrusters power on logic deadzone appropriately, system oscillations generated by opening and closing the RCS thrusters frequently can be avoided. The six degrees of freedom simulation results are presented to show the efficiency of the designed control law.*

Keywords: Aircraft control, Near space, Compound control, Reaction control system (RCS)

1. **Introduction.** Near space, between the static ceiling of general fighters and the lowest height of orbiters, has not been exploited much by human beings before even though it is of significance for many practical applications. With the rapid development of science and technology, near space has been one of the hottest research fields in many countries (see, for example, [1, 2, 3, 4, 5, 6, 7] and the references therein).

It is well known that an elevator provides low efficiency or sometimes fails due to rarefied air and poor performance of the thrust systems, which cannot provide thrust vectors. RCS is one of main control methods to solve the problem, which is a thrust control system consisting of several thrusters to produce rolling, pitching and yawing moments [8]. An RCS system is capable of providing a small amount of thrust in any desired direction or combination of directions. An RCS system is also capable of providing torque to allow the control of rotation (pitch, yaw, and roll). Compared with a spacecraft's main engine, which only provides thrust in one direction, RCS is much more powerful. As a consequence, the RCS method has received much attention in recent decades. For example, [9] presents an Adaptive Pulse Modulator (APM) thruster selection algorithm, which provides the capability to exploit all of the available thruster control power. The APM algorithm can use any subset of the RCS thrusters, which can autonomously adapt

to vehicle/thruster dispersions, and adapt to thruster failures. [10] presents the design of lateral/directional control with RCS on reentry of Reusable Launch Vehicle. The control law is designed for a linear system and then applied in a nonlinear way with on-off type RCS. [11] develops a controller for using the forward reaction control system jets as an additional control during entry, and assesses its value and feasibility during failure situations. Forward-aft jet blending logic is created and implemented on a simplified model of the space shuttle entry flight control system. Other RCS methods developed incorporate various control theories can be found in [12, 13, 14] and so on. So far, most RCS methods are used for reusable launch vehicle (RLV), and there are few RCS design results for near space vehicles with the situation of rarefied air and aerodynamic rudder failure. For near space vehicles, how to design the RCS compound control law to improve the system performance and avoid the saturation problem of the elevators still needs to be investigated.

Usually, a near space vehicle is launched by an airplane with the assistance of a rocket. For example, during the launching process of X-43 aircraft, a winged booster rocket with the X-43 itself at the tip, called a "stack", is launched from a carrier plane B-52 [15]. After the booster rocket brings the stack to the target speed and 29 kilometers high altitude, it is discarded, and the X-43 flies freely using its own engine, a scramjet, and starting the cruising stage.

Since the air in 20 kilometers altitude is rarefied, an aircraft can inertially climb in virtue of the kinetic energy of the booster rocket and then adjust its attitude at a certain height to start cruising or diving to the target according to different tasks. Due to the rarefied air, the rudder efficiency decreases, and thus maneuvering requirement cannot be met only by pneumatic rudder-control.

Since little rolling action and yawing action are necessary, the pitch loop is the key design to control the vehicle. The main aim of this paper is to design the control law for the pitch loop. The rest of this paper is organized as follows. Section 2 describes the state-space mode of a near space vehicle with small disturbance linearization and presents the classic PID control law. In Section 3, we propose RCS configuration modes and the compound control method of the elevator. In Section 4, simulation results are presented to show the effectiveness of the improved compound control method.

2. **Problem Formulation.** Subject to the constraints of 40 kilometers height, 3 Mach flight speed and 8 degrees attack angle, the state-space function of a near-space vehicle under small disturbance linearization can be described by:

$$\begin{bmatrix} \Delta\dot{q} \\ \Delta\dot{w} \\ \Delta\dot{u} \\ \Delta\dot{\theta} \end{bmatrix} = \begin{bmatrix} -0.067 & -0.002 & 0 & 0 \\ 100.8 & -0.052 & -0.007 & -4.709 \\ -70.46 & 0.003 & -0.001 & -8.495 \\ 1 & 0 & 0 & 0 \end{bmatrix} \begin{bmatrix} \Delta q \\ \Delta w \\ \Delta u \\ \Delta\theta \end{bmatrix} + \begin{bmatrix} -1.195 \\ -2.286 \\ 0.015 \\ 0 \end{bmatrix} \Delta\delta_e, \quad (1)$$

where Δq is the increment of pitching angular velocity; Δw is the velocity increment in z axis direction of body coordinate system; Δu is the velocity increment in x axis direction of body coordinate system; $\Delta\theta$ is the pitching angular increment; $\Delta\delta_e$ is the elevator deflection angular increment. The inner loop control law is designed as:

$$\delta_{ec} = K_p^\delta(\Delta r + K_I^\delta \int \Delta r dt) + K_\alpha^\delta \alpha + K_q^\delta \frac{1}{1+\tau_q s}\dot{\theta}, \quad (2)$$

where Δr is the difference between the outer loop instruction r_c and the instruction feedback r_b; α is the flight attack angle; θ is pitching angle; $\dfrac{1}{1+\tau_q s}$ is the lowpass filter with the time constant τ_q designed as 0.1; K_p^δ, K_I^δ, K_α^δ and K_q^δ are the designed parameters

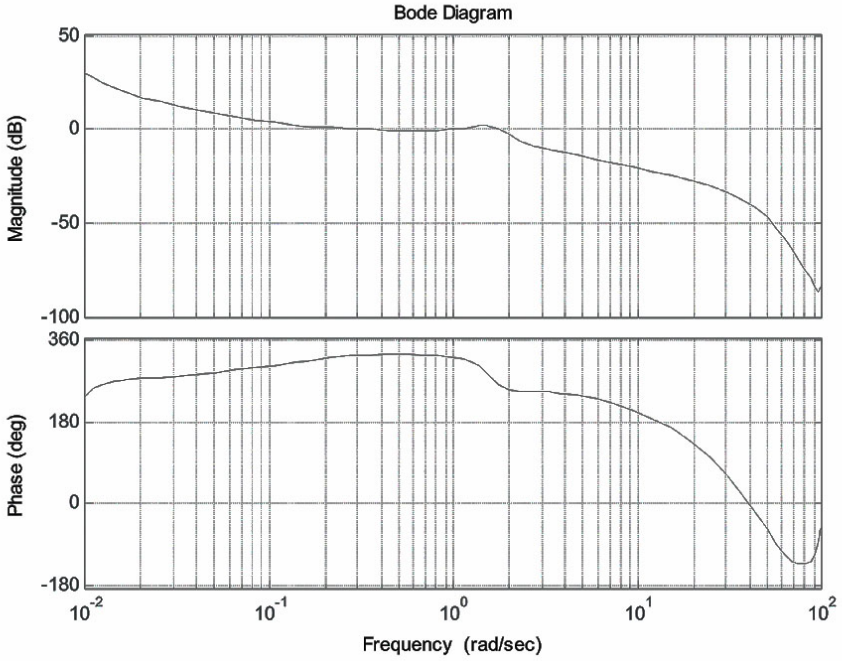

FIGURE 1. The Bode diagram of system with control law

of the inner loop control law, which are -0.8, 2, -0.2, 0.5; δ_{ec} is the command input of the elevator, the dynamic relationship between δ_{ec} and the real deflection angle of an elevator can be expressed approximately as:

$$W_{\delta_{ec}}^{\delta_c} = \frac{2500}{S^2 + 75S + 2500}. \tag{3}$$

The outer loop control law is:

$$r_c = K_P^h (h_c - h) - K_D^h \dot{h} - K_q^h \dot{\theta}, \tag{4}$$

where h_c is the command height; h is the real flight height; K_p^h, K_D^h and K_q^h are the design parameters of outer loop control law, which are -1.2, 0.6, 0.4. The Bode diagram of the system with control law is shown as Figure 1.

Figure 1 shows that the phase stability margin is 82.8 degrees and the amplitude stability margin is 23.4 dB.

In the design course of the above control law, the limit range of the elevator is not considered. The moment M_{δ_e} should satisfy

$$M_{\delta_e} = m_z^{\delta_e} q_c S L \delta_e, \tag{5}$$

where $m_z^{\delta_e}$ is the rudder effectiveness of the elevator; S is the characteristic area of the aircraft; L is the characteristic length of the aircraft; and q_c is the dynamic pressure satisfying:

$$q_c = \frac{1}{2}\rho\nu^2, \tag{6}$$

where ρ is the air density of the position of the aircraft; ν is the flight speed of the aircraft. Due to the high flight speed, the rarefied air and the low dynamic pressure, the elevator cannot produce enough moment to accomplish attitude adjustment of the aircraft. The six degrees of freedom simulation curve is shown in Figure 2. Figure 2(a) shows the

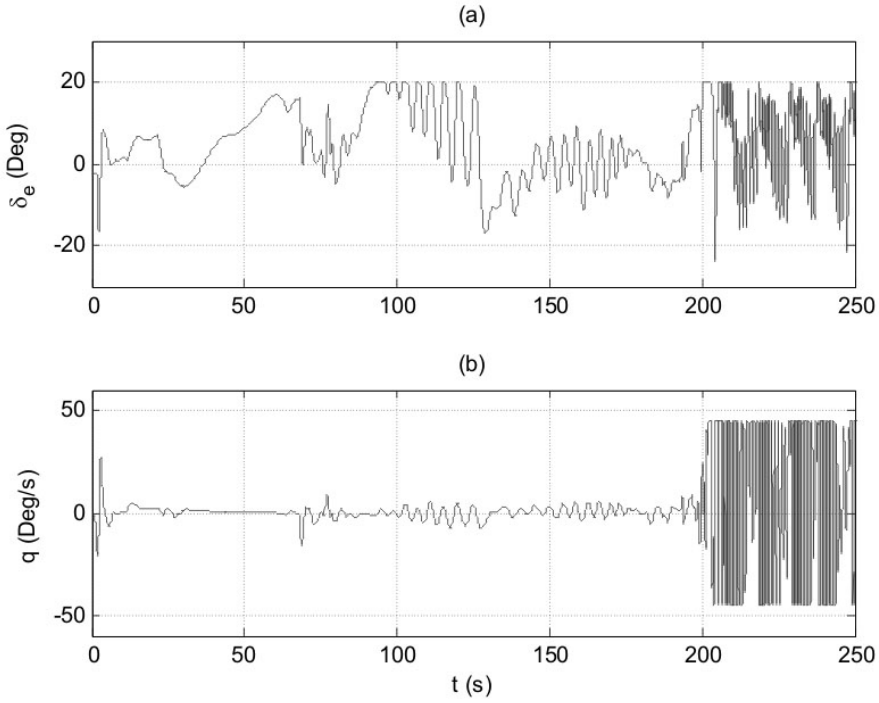

FIGURE 2. The simulation curves without RCS

simulation curve of the deflection angle δ_e of the elevator, and Figure 2(b) shows the simulation curve of the pitching angular velocity.

We can see from Figure 2(a) that the elevator reaches the saturation at about 93 seconds (when the aircraft climbs to about 36.5 kilometers) such that the elevator cannot provide enough moment to adjust the attitude of aircraft. Then, the system starts to oscillate and finally goes to divergence.

3. **RCS Compound Control.** In order to conquer the saturation problem of the elevator in Section 2, we propose the compound control method of the elevator and RCS configurations.

3.1. **RCS configuration.** An RCS has many configuration modes. Reasonable configuration can play full role and will help the aerodynamic rudder to achieve the desired control result.

Scheme 1 in Figure 3 applies 8 thrusters with their fittings and pipelines, four of which are installed on four borders of the aircraft tail, where the force direction passes over the projection point of the aircraft centroid on the tail cross section; the other four thrusters are installed in the four corners, where the force direction passes over the projection point of the aircraft centroid on the tail cross section. The advantage of this scheme is that it is easy to combine and operate; and the disadvantage of this scheme is that there exists less thrust grade provided by the thruster and fault reconstruction ways, i.e., this scheme can provide limited rolling moment.

The thruster combination logic of scheme 1 is shown in Table 1.

Scheme 2 in Figure 4 applies 10 thrusters with their fittings and pipelines, two of which are installed on upper and lower borders of the aircraft tail, where the force direction passes over the projection point of the aircraft centroid on the tail cross section; the other eight thrusters are installed in the endpoints of lower and upper borders in pairs, where the force direction is perpendicular to the connecting line between the force point and the

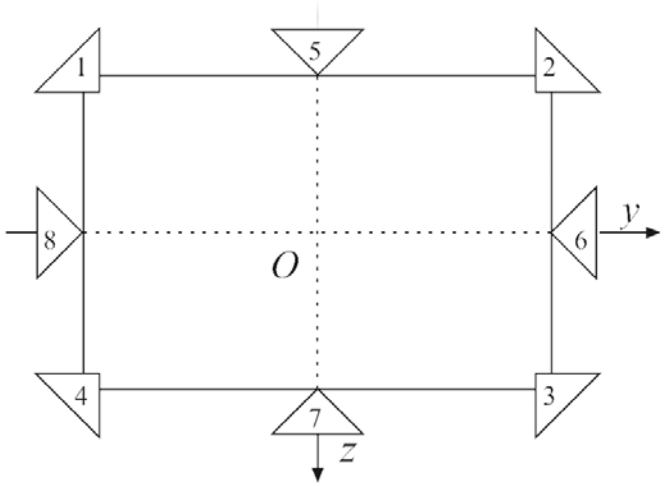

FIGURE 3. The RCS thruster configuration of scheme 1

TABLE 1. The thruster combination logic of scheme 1

Action	Direction	Engine
Roll	Positive	Null
Roll	Negative	Null
Pitch	Positive	5OR1&2OR1&2&5
Pitch	Negative	7OR3&4OR3&4&7
Yaw	Positive	6OR2&3OR2&3&6
Yaw	Negative	8OR1&4OR1&4&8

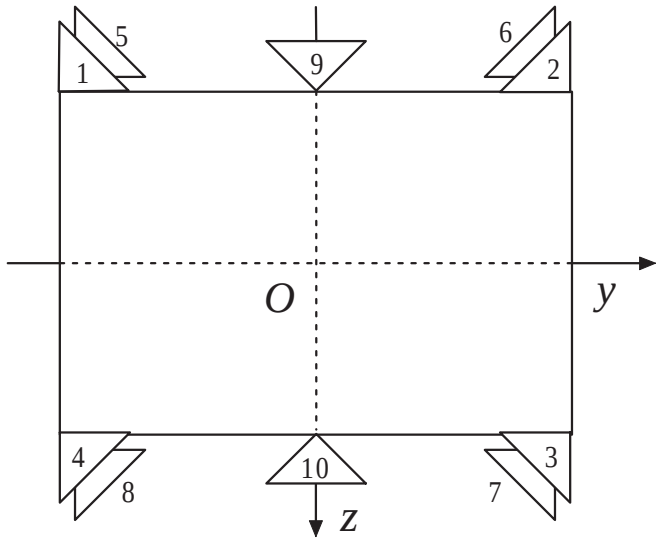

FIGURE 4. The curve of scheme 2 of RCS

projection point of the aircraft centroid on the tail cross section. The advantage of this scheme is that these exists more combination ways and fault reconstruction ways, thus the adjustment of rolling moment is strong; the disadvantage of this scheme is that with the increase of the thrusters, resulting that the design of control logic becomes complicated.

TABLE 2. The thruster combination logic of scheme 2

Action	Direction	Engine
Roll	Positive	2(6)&4(8)OR 2&4&6&8
Roll	Negative	1(5)&3(7)OR 1&3&5&7
Pitch	Positive	9OR1(5)&2(6)OR1(5)&2(6)&9 OR1&2&5&6 OR1&2&5&6&9
Pitch	Negative	9OR1(5)&2(6)OR1(5)&2(6)&9 OR1&2&5&6 OR1&2&5&6&9
Yaw	Positive	1(5)&4(8)OR 1&5&4&8
Yaw	Negative	2(6)&3(7)OR 2&6&3&7

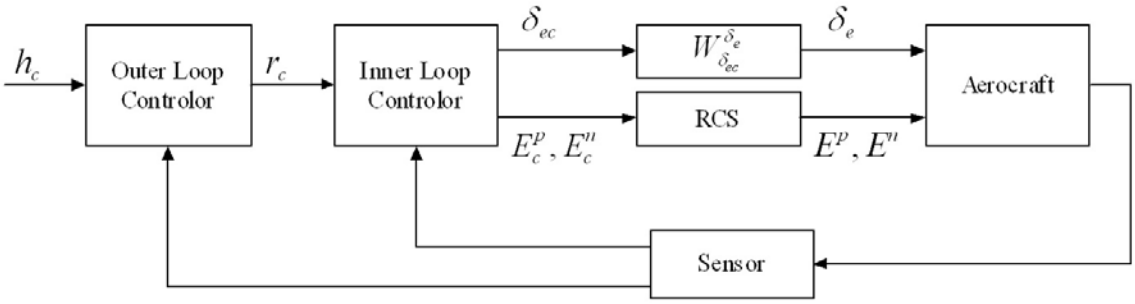

FIGURE 5. The elevator and RCS compound control law

The thruster combination logic of scheme 2 is shown in Table 2. By comparing Table 1 and Table 2, we find that the thrusters of scheme 2 have more combination ways and more fault reconstruction ways. For example, if thruster 1 in scheme 1 fails, mode 1&2 and 1&2&5 cannot provide pitching motion, which can be achieved only by thruster 5, when only one thruster level is provided. In scheme 2, if thruster 1 fails, thruster 9, mode 5&2(6) and mode 5&9&2(6) can produce the pitching motion.

3.2. **Design of the elevator and RCS compound control law.** By using RCS compound control, the control law structure of the system is shown in Figure 5. Here E^p_c is the RCS thruster boot-strap logic instruction value, which produces a positive pitching moment; E^n_c is the RCS thruster boot-strap logic instruction value, which produces a negative pitching moment; E^p is the thrust produced by RCS thruster, which provides a positive pitching moment; E^n is the thrust produced by RCS thruster, which provides a negative pitching moment. It takes a course for the RCS thrust produced by the thruster from zero to existence and from existence to zero. The dynamic process is approximated as rate limiter [2], that is

$$E^p = \begin{cases} F_E(t-t_0)/\tau & \text{when } t_0 \le t < t_0+\tau \\ F_E/\tau & \text{when } t_0+\tau \le t < t_f \\ F_E(t_f+\tau-t)/\tau & \text{when } t_f \le t < t_f+\tau \\ 0 & \text{when other,} \end{cases} \tag{7}$$

where F_E is the maximum thrust produced by RCS thruster, which is 375N given by run test; t_0 is the starting time of RCS thruster; t_f is the closing time of RCS thruster; τ is a delay time when the thrust produced from zero to existence and from existence to zero, which is 0.2 second given by run test. The dynamical relationship of E^n is almost the same, except that the sign is reverse to the case of F_E. With the compound control, RCS thruster power on logic E^p_c, which produces positive pitching moment, satisfies

$$E^p_c = \text{relay}\left(-\delta_e \,\middle|\, \left[-\delta^p_e,\ -\delta^{\text{sub}}_e\right]\right), \tag{8}$$

where relay $(x\,|[\underline{x},\bar{x}])$ is deadzone function with $\underline{x}<\bar{x}$. When $x\geq\bar{x}$, the output of the system is 1; when $x\leq\underline{x}$, the output of the system is 0; when $x\in(\underline{x},\bar{x})$, the output keeps the original value. If there is no output before, set the output as 0. δ_e^p is the elevator defection when RCS thruster is closed, which produces positive pitching moment; δ_e^{sub} is the negative maximum deflection angle of the elevator; interval $\left[\delta_e^{\text{sub}},\delta_e^p\right]$ is the power on logic deadzone of RCS thruster, which produces the positive pitching moment. With the compound control, the power on logic E_c^n of RCS thruster, which produces positive pitching moment, satisfies

$$E_c^n=\text{relay}\left(\delta_e\,|[\delta_e^n,\ \delta_e^{\text{sup}}]\right), \tag{9}$$

where δ_e^n is the elevator deflection angle when the RCS thruster is closed, which produces negative pitching moment; interval $[\delta_e^n,\delta_e^{\text{sup}}]$ is power on logic deadzone of RCS thruster, which produces negative pitching moment. With the compound control, the elevator instruction is

$$\delta_{ec}=K_P^\delta\left(\Delta r+K_I^\delta\int\Delta r\mathrm{d}t\right)+K_\alpha^\delta\alpha+K_q^\delta\frac{1}{1+\tau_q s}\dot{\theta}-K_E^\delta\left(E_c^n-E_c^p\right), \tag{10}$$

where K_E^δ is the design proportional parameter.

The power on the logic deadzone of the RCS thruster should not be too large, otherwise the moment produced by the elevator will cancel out the moment produced by RCS thrust, resulting that control efficiency drops. At the same time, the RCS thruster power on logic deadzone should not be too small; otherwise, the RCS thruster will open and close frequently, resulting that the system oscillates.

Figure 6 is the simulation curve with the logic deadzone of the RCS thruster set as $[17,20]$, where the RCS thruster produces a negative pitching moment. Figure 6(a) shows the simulation curve of the RCS thruster pitching moment; Figure 6(b) shows the simulation curve of the elevator deflection angle; Figure 6(c) shows the simulation curve of the pitching angular velocity. The simulation curves show that since the logic deadzone is set too small, the RCS thruster open and close frequently, resulting oscillation of the pitching angular velocity.

4. **Simulations.** The simulation curves of the flight height, velocity and dynamic pressure with the elevator and RCS compound control are shown in Figure 7. Figure 7(a) shows the flight height of the aircraft, Figure 7(b) is the simulation curve of the flight Mach, and Figure 7(c) is the flight dynamic pressure curve with sensor feedback. These curves show that when the aircraft flights to certain velocity with the booster rocket, the booster rocket stops working and the aircraft climbs by inertia, when kinetic energy is transformed into potential energy and the flight height increases with decreasing velocity. Since the air density is falling and the flight velocity is dropping at 4 kilometers high, the dynamic pressure of aircraft is low.

Figure 8 shows the simulation curve of the pitching moment, the elevator deflection angle and the pitching angular velocity produced by RCS with the compound control of the elevator, where Figure 8(a) is the simulation curve of the pitching moment produced by RCS; Figure 8(b) is the simulation curve of the elevator deflection angle; Figure 8(c) is the pitching angular velocity curve. Figure 8 shows that when the flight height is close to the maximal point and the flight dynamic pressure is low, the elevator deflection angle achieves to saturation. However, by the proposed RCS compound control, the elevator efficiency is rationally compensated and the aircraft can flight according to the scheduled flight path.

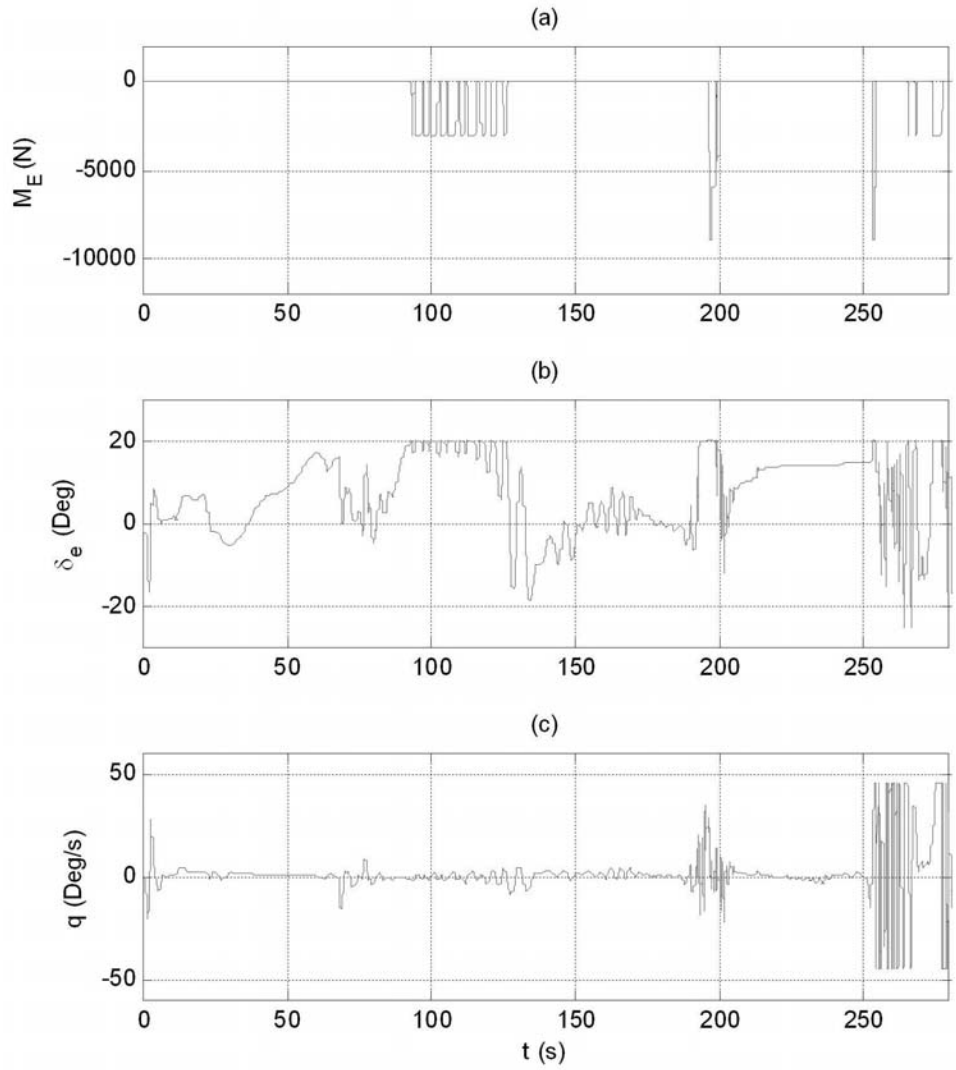

FIGURE 6. The simulation curves of the RCS thruster pitching moment, the elevator deflection angle and the pitching angular velocity with small logic deadzone

In this simulation, the power on logic deadzone of the RCS thruster, which produces negative pitching moment, is set as $[10, 20]$, and the power on logic deadzone of the RCS thruster, which produces positive pitching moment, is set as $[-30, -15]$.

5. **Conclusions.** In this paper, by analyzing the elevator saturation reason, we presented the elevator and RCS compound control scheme for a kind of near space vehicles and showed the characteristic analysis of two RCS configuration schemes. A reasonable control scheme could be chosen according to the general design requirement of the aircrafts. By the proposed RCS, the rudder saturation problem is solved, which is produced by rudder efficiency of the elevator decreasing under low dynamic pressure. The six degrees of freedom simulations show the efficiency of the proposed control method.

Acknowledgment. This work was supported by a 973 project (2011CB707005). This work was also partially supported by the National Natural Science Foundation of China under Grant (No. 11171079), the Australian Research Council discovery projects, JSPS Research Fellowship, and Japanese Grant-in-Aid for Scientific Research under Grant (No. 2200800).

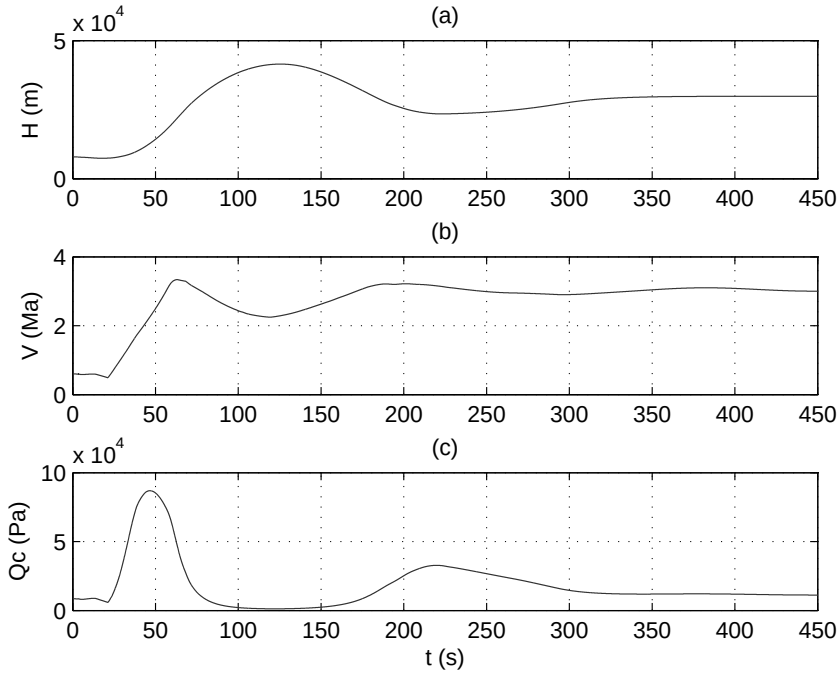

FIGURE 7. The simulation curves of fight height, flight velocity and dynamic pressure

REFERENCES

[1] E. R. Moomey, *Technical Feasibility of Loitering Lighter than Air Near Space Maneuvering Vehicles*, Air Force Institute of Technology, Wright-Patterson AFB, Ohio, USA, 2005.

[2] Y. Sun, Application analysis and prospects of near-space vehicles, *Radio Engineering of China*, vol.38, pp.26-28, 2008.

[3] E. B. Tomme and S. J. Dahl, Balloons in today's military – An introduction to the near-space concept, *Air and Space Power Journal*, vol.19, pp.39-49, 2005.

[4] D. Wegerif, D. Rosinski and W. Parton, Whole arm proximity control system for articulated robots working near space vehicles and flight hardware, *Space Programs and Technologies Conference and Exhibit*, AIAA-93-4158, Huntsville, AL, USA, pp.21-23, 1993.

[5] Y. Marcus and K. Stephanie, An overview of advanced concepts for near-space systems, *Technical Report*, AIAA-2009-4805, 2009.

[6] G. Cai, G. Duan and C. Hu, A velocity-based LPV modeling and control framework for an airbreathing hypersonic vehicle, *International Journal of Innovative Computing, Information and Control*, vol.7, no.5(A), pp.2269-2281, 2011.

[7] Y. Xu, B. Jiang, G. Tao and Z. Gao, Fault accommodation for near space hypersonic vehicle with actuator fault, *International Journal of Innovative Computing, Information and Control*, vol.7, no.5(A), pp.2187-2200, 2011.

[8] G. E. Funk and R. M. Stephenson, On orbit shuttle/mir mated RCS and crew load analyses, AIAA-97-1041, 1997.

[9] T. A. Claggett, D. W. Brekke and R. D. Jones, A health-optimal adaptive reaction control system for spacecraft, *2011 IEEE Aerospace Conference*, Big Sky, MT, USA, pp.1-13, 2011.

[10] L. Wu, Y. Huang and C. He, Lateral-direction control via reaction control system, *2009 International Asia Conference on Informatics in Control, Automation and Robotics*, Milan, Italy, pp.52-56, 2009.

[11] C. Restrepo and J. Valasek, Preliminary study using forward reaction control system jets during space shuttle entry, *AIAA Conference and Exhibit on Guidance, Navigation, and Control*, Keystone, CO, USA, pp.1-10, 2006.

[12] A. D. Rosello, *A Vehicle Health Monitoring System for the Space Shuttle Reaction Control System During Reentry*, MIT, 1995.

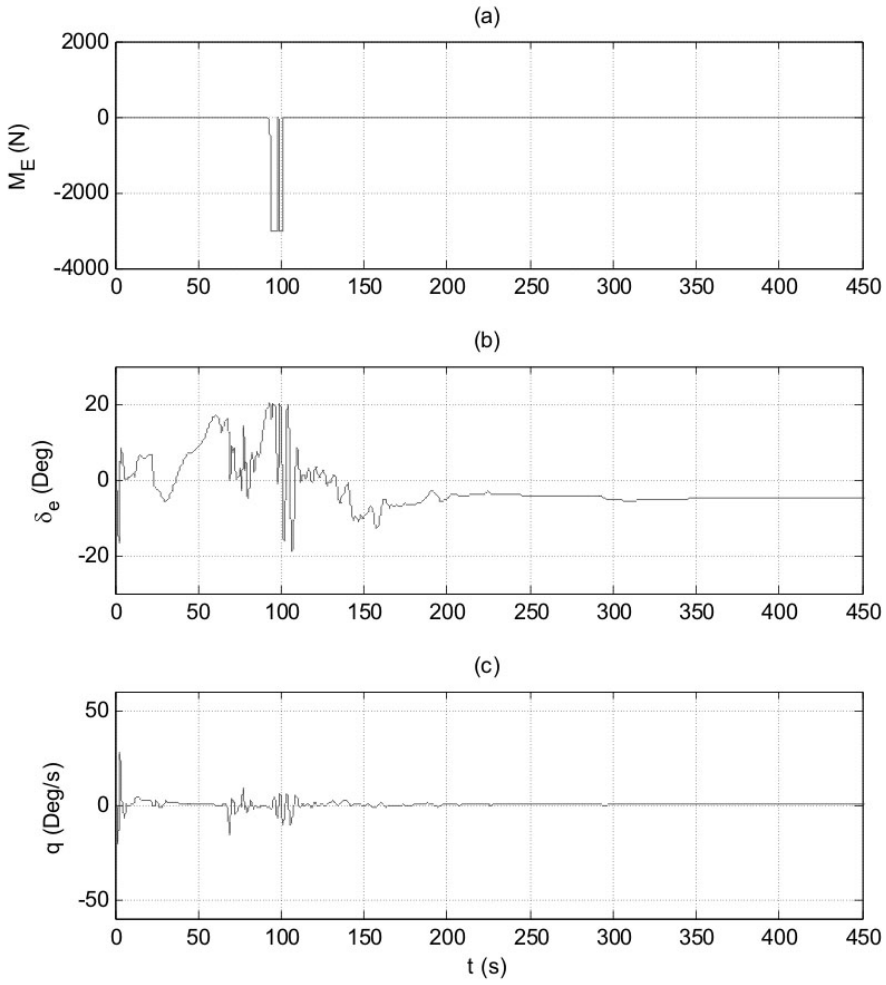

FIGURE 8. The simulation curves of RCS moment, the elevator deflection angle and pitching angular velocity

[13] T. Ting and N. Flanagan, Space shuttle transition controller OMS-TVC and RCS jet thruster stability analysis, *The 27th Joint Propulsion Conference of AIAA, SAE, ASME, and ASEE*, Sacramento, CA, USA, AIAA-91-2220, 1991.

[14] G. D. Ning, S. G. Zhang and Z. P. Fang, Research on the reaction control system for spacecraft re-entry flight, *Flight Dynamics*, vol.23, pp.16-19, 2005.

[15] P. T. Harsha, M. L. C. Keel and A. Castrogiovanni, X-43A vehicle design and manufacture, *The 13th International Space Planes and Hypersonics Systems and Technologies of AIAA/CIRA*, Capua, Italy, pp.1-9, 2005.